

Long-Lived Slepton in the Coannihilation Region and Measurement of Lepton Flavour Violation at LHC

S Kaneko^{1, 2}, J Sato³, T Shimomura⁴, O Vives⁴, M Yamanaka³

¹Instituto Física Corpuscular - C.S.I.C./Universitat de València Campus de Paterna, Apt 22085, E46071, València, Spain

² CFTP, Departamento de Física Instituto Superior Técnico, Avenida Rovisco Pais, 1 1049-001 Lisboa, Portugal

³ Department of Physics, Saitama University, Shimo-Okubo, Sakura-ku, Saitama, 338-8570, Japan

⁴ Departament de Física Teòrica and IFIC, Universitat de València - CSIC, E46100, Burjassot, València, Spain

Abstract. When the mass difference between the lightest slepton and the lightest neutralino is smaller than the tau mass, the lifetime of the lightest slepton in the constrained Minimal Supersymmetric Standard Model (MSSM) increases in many orders of magnitude with respect to typical lifetimes of other supersymmetric particles. In a general MSSM, the lifetime of the lightest slepton is inversely proportional to the square of the intergenerational mixing in the slepton mass matrices. Such a long-lived slepton would produce a distinctive signature at LHC and a measurement of its lifetime would be relatively simple. Therefore, the long-lived slepton scenario offers an excellent opportunity to study lepton flavour violation at ATLAS and CMS detectors in the LHC and an improvement of the leptonic mass insertion bounds by more than five orders of magnitude would be possible.

1. Introduction

Cosmological observations have confirmed the existence of the non-baryonic dark matter. The observed dark matter relic abundance ($\Omega_{DM}h^2 \simeq 0.11$) suggests the existence of a stable and weakly interacting particle with a mass 100 – 1000 GeV. In supersymmetric (SUSY) models with conserved R-parity, the Lightest Supersymmetric Particle (LSP), usually the lightest neutralino, is stable and is a perfect candidate for the dark matter. In fact, although the dark matter abundance at an arbitrary point of the SUSY parameter space is usually too large, the observed abundance can be reached in regions where the LSP abundance is effectively lowered by annihilation. One of the mechanisms to lower the dark matter abundance is the so-called coannihilation [1]. In the coannihilation region, the Next to Lightest Supersymmetric Particle (NLSP) has a mass nearly degenerate to the LSP. Then the NLSP and the LSP decouple from thermal bath almost simultaneously and the LSP annihilates efficiently through collisions with the NLSP. The degeneracy required for the coannihilation to occur is generally $\delta m/m_{LSP} < \text{a few } \%$, where $\delta m = m_{NLSP} - m_{LSP}$.

In addition, it was pointed out in [2, 3, 4] that if staus are the NLSP and its mass difference with the LSP is less than the tau mass, they destroy ${}^7\text{Li}/{}^7\text{Be}$ nucleus through the internal conversion during Big-Bang Neucleosynthesis (BBN). With this small mass difference, staus become long-lived and survive until BBN starts. Then, they form bound states with nucleus. The stau-nucleus bound states decay immediately by virtual exchange of the hadronic current. In this way, the relic abundance of the light elements is lowered effectively and the discrepancy between the observed value of ${}^7\text{Li}/{}^7\text{Be}$ abundance [5, 6] and the predicted value from the standard BBN [7] with WMAP data [8, 9] can be solved. Thus, a scenario with stau NLSP and neutralino LSP with $\delta m \leq m_\tau$ could explain the relic abundance of the light elements as well as the abundance of the dark matter.

Strictly speaking, the above discussion is true only in the framework of the MSSM without intergenerational mixing in the slepton sector. However, in a general MSSM, we naturally expect some degree of intergenerational mixing in the sfermion sector. For example, even if we start from a completely universal MSSM at the GUT scale in the presence of neutrino Yukawa couplings, a small mixing between different sleptons is generated by renormalization group equations. Moreover, there is no fundamental reason to restrict the flavour structures to the Yukawa couplings and keep the soft mass matrices universal. In fact, we would expect the same mechanism responsible for the origin of flavour to generate some flavour mixing in the sfermion sector. In general, we expect that the lightest slepton, \tilde{l}_1 , is not a pure stau, but there is some mixing with smuon and selectron. In the presence of this small intergenerational mixing, even with $\delta m \leq m_\tau$, other two-body decay channels like $\tilde{l}_1 \rightarrow \tilde{\chi}_1^0 + e(\mu)$, are still open [2]. In this case, given that the flavour conserving two-body decay channel is closed, the slepton lifetime will have a very good sensitivity to small Lepton Flavour Violation (LFV) parameters. The lifetime will be inversely proportional to the sfermion mixing until two-body decay width becomes comparable to three or four-body decay widths. Thus, it is worthwhile to study the lifetime of the sleptons in small δm case to obtain information on LFV parameters. Several papers have studied the possibility of measuring LFV at colliders [10, 11, 12, 13, 14, 15, 16, 17]. However, in these papers the LFV decays are always subdominant with small branching ratios and is never possible to reach the level of sensitivity we reach in our scenario. Only Ref. [14] considers LFV in e^+e^- colliders through the slepton production in a long-lived stau scenario in a gauge-mediated model and as in the other works they are not sensitive either to the presence of small lepton flavour violation that we consider in this paper.

Long-lived charged-particles are very interesting since they provide a clear experimental signature at the LHC [18, 19, 20]. In Ref. [21], it is concluded that even if the lifetime of the decaying particle is much longer than the size of the detector, some decays always take place inside the detector and it is possible to measure lifetimes as long as $10^{-5} - 10^{-3}$ seconds in a particular gauge mediation scenario.

2. Long-lived Stau in MSSM

We start the analysis looking for allowed regions in the Constrained MSSM (CMSSM) parameter space where the difference, δm , between the lightest neutralino mass, $m_{\tilde{\chi}_1^0}$, and the lighter stau mass, $m_{\tilde{\tau}_1}$, is smaller than the tau mass, m_τ . In this section, we consider the case of a CMSSM defined at the GUT scale without neutrino Yukawa couplings. Then, $\tilde{\tau}_1$ is equal to a combination of only the right and left-handed stau. The CMSSM is parametrized by 4 parameters (the universal gaugino masses, $M_{1/2}$, the universal scalar masses, m_0 , the universal trilinear couplings, A_0 , at the GUT scale and the ratio of vacuum expectation values of two Higgses, $\tan\beta$) and

one sign (of μ). In our numerical analysis, we use SPheno [22] and micrOMEGAs [23] to obtain mass spectrum at electroweak scale and relic dark matter abundance.

First, we list the experimental constraints used in our analysis. The main constraint, apart from direct limits on SUSY masses, comes from the relic density of the dark matter abundance reported by WMAP collaboration. Although the latest data is obtained in [9], we use more conservative range in this paper, $0.08 < \Omega_{\text{DM}} h^2 < 0.14$, but the results would be basically the same as the one with a narrower range.

A second constraint comes from the anomalous magnetic moment of the muon, $a_\mu = (g - 2)_\mu/2$, that has been measured precisely in the experiments at BNL [24]. The difference between the experiment and the standard model prediction is given [25] as $\Delta a_\mu = a_\mu^{(\text{exp})} - a_\mu^{(\text{SM})} = (27.5 \pm 8.4) \times 10^{-10}$, which corresponds to a difference of 3.3 standard deviations. These results seem to require a positive and sizable SUSY contributions to a_μ , although it is still not conclusive. In the following, in all our plots we will show the regions favored by measurement of a_μ at a given confidence level, but we will not use it as a constraint to exclude the different points. The bound on $\text{Br}(b \rightarrow s\gamma)$ is also taken into account, but as we will see, in the region of small δm and correct dark matter abundance, $M_{1/2} \geq 700$ GeV. Therefore the numerical prediction we obtained for $\text{Br}(b \rightarrow s\gamma)$ is always very close to the SM predictions.

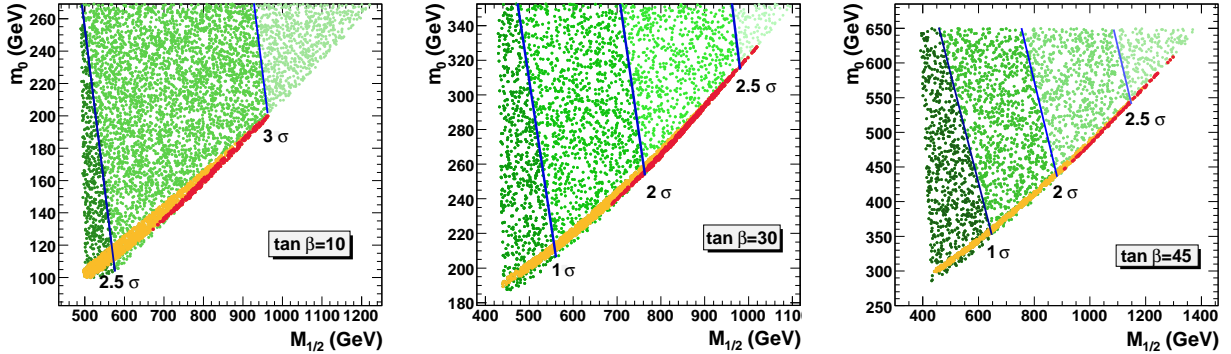


Figure 1. The allowed parameter regions in $M_{1/2} - m_0$ plane fixing $A_0 = 600$ GeV. $\tan \beta$ is varied 10, 30, 45 shown in each figure. The red (dark) narrow band is consistent region with dark matter abundance and $\delta m < m_\tau$ and the yellow (light) narrow band is that with $\delta m > m_\tau$. The green regions are inconsistent with the dark matter abundance, and the white area is stau LSP region and excluded. The favored regions of the muon anomalous magnetic moment at 1σ , 2σ , 2.5σ and 3σ confidence level are indicated by solid lines.

In Fig. 1, we show the allowed parameter regions in the $M_{1/2} - m_0$ plane for $\tan \beta = 10, 30, 45$ and $A_0 = 600$ GeV. The sign of μ is taken to be positive in all figures as required by the $b \rightarrow s\gamma$ and a_μ constraints. In these figures, the solid lines indicate the different confidence level regions for the a_μ constraint. The yellow (light) narrow band is the region with correct dark matter abundance corresponding to the coannihilation region and with $\delta m > m_\tau$. The red (dark) band in the coannihilation region represents the points with correct dark matter abundance and $\delta m < m_\tau$. The green regions are not consistent with the dark matter abundance while the white area is the stau LSP region and therefore is excluded. Note that in models where the observed

dark matter abundance is accounted for other dark matter components besides the neutralino, the small δm region could be extended to the green regions below the yellow band. Notice that choosing a positive and large A_0 ($\lesssim 3m_0$), the renormalization group evolved value $A(M_W)$ is reduced with respect to the cases of zero or negative A_0 . Therefore the left-right entry in the stau mass matrix, $A - \mu \tan \beta$, is also reduced. Then the region of neutralino LSP, for a fixed value of the neutralino mass, $m_{\tilde{\chi}_1^0}$ ($\simeq 0.4M_{1/2}$), corresponds to smaller values of m_0 for positive A_0 than for zero or negative A_0 . Therefore this implies slightly lighter spectrum and larger contributions to a_μ . From these plots we can see that the interesting region of correct value of dark matter relic abundance and $\delta m < m_\tau$ corresponds always to relatively large values of $M_{1/2}$. This is due to the fact that the coannihilation cross section decreases at larger SUSY masses [26] and for sufficiently large $M_{1/2}$ the cross section is too small to produce a correct dark matter abundance, even for $m_{\tilde{\tau}_1} \simeq m_{\tilde{\chi}_1^0}$.

Comparing the different $\tan \beta$ values, we can see that at low $\tan \beta$ the long-lived stau region corresponds to smaller values of $m_0 \sim (120, 200)$ GeV, although it can only reach the a_μ favored region at 3σ . For $\tan \beta = 30$, the long-lived stau region corresponds to similar values of $M_{1/2}$, but the required values of m_0 are nearly a factor two larger. However, in this case the larger value of $\tan \beta$ allows this region to reach the a_μ favored region at the 2σ level. At $\tan \beta = 45$ the long-lived stau region corresponds to larger values of both $M_{1/2}$ and m_0 and it can only reach the a_μ favored region at 2.5σ . This behavior of the allowed regions can be understood as follows. Since the SUSY contribution to a_μ is proportional to $\tan \beta / m_{\tilde{\chi}_1^0}^2$, it is small when $\tan \beta = 10$. But it is also suppressed at $\tan \beta > 30$ because the mass of the neutralino becomes heavier for large $\tan \beta$. With fixed A_0 , the neutralino mass is determined mainly by $M_{1/2}$ and the increase of the neutralino mass according to the increase of $\tan \beta$ is seen in Fig. 1.

The decay rates of the NLSP stau into two, three and four bodies are approximately given in [27]. Notice that when $\delta m \gtrsim m_\tau$ the two-body decay is open and the lifetime of the stau, $\tau_{\tilde{\tau}_1}$, is $\lesssim 10^{-22}$ sec. However, for $\delta m \lesssim m_\tau$ this decay is closed and the three or four-body decays are suppressed at least by an additional $(\delta m)^4 G_F^2 (f_\pi/m_\tau)^2 1/(30(2\pi)^2) \simeq 10^{-13}$ with $\delta m \sim 2$ GeV. Therefore the stau becomes long-lived and the phenomenology of the MSSM changes dramatically.

3. LFV and Long-lived Slepton

In the previous section, we have seen that $\delta m \leq m_\tau$ is indeed possible in a CMSSM without LFVs. As was shown in [2], the lifetime of the NLSP stau increases by many orders of magnitude. However, in realistic models, we expect a certain degree of intergenerational mixing to be present in the slepton sector. Once a new source of LFVs is introduced, the NLSP two-body decay channels into electron and/or muon is open again. In this case, the lifetime is inversely proportional to the square of the mixing of selectron and smuon with stau and therefore the measurement of the lifetime shows a strong sensitivity to LFV parameters. In this section, we show the dependence of the lifetime of the lightest slepton on the right-handed and the left-handed slepton mixings. All the numerical results of lifetimes and figures presented below are calculated using the exact formula given in [27].

To understand the dependence of lifetimes on LFV parameters, it is convenient to introduce the so-called Mass Insertions (MI), $(\delta_{RR/LL}^e)_{\alpha\beta}$, defined in the same way as [27]. In terms of

Table 1. Table of the mass difference and the lightest slepton, neutralino masses. m_0 , A_0 and $\tan\beta$ are fixed to 260 GeV, 600 GeV and 30, respectively. The values of neutralino abundance and a_μ are shown for the reference.

No.	δm (GeV)	$m_{\tilde{\chi}_1^0}$ (GeV)	$m_{\tilde{l}_1}$ (GeV)	$\Omega_{\tilde{\chi}_1^0} h^2$	$a_\mu (\times 10^{-10})$
A	2.227	323.1549	325.3817	0.110	10.32
B	1.650	325.5601	326.2147	0.102	10.25
C	0.407	327.6294	328.0365	0.085	10.09
D	0.092	328.4060	328.4981	0.081	10.06

these mass insertions, the two-body decay rate is approximately given by

$$\Gamma_{2\text{-body}} = \frac{g_2^2}{2\pi m_{\tilde{\tau}_1}} (\delta m)^2 (|g_{1\alpha 1}^L|^2 + |g_{1\alpha 1}^R|^2), \quad (1)$$

where $\alpha = e, \mu$. $g_{1\alpha 1}^{L,R}$ can be approximated in the mass insertion as shown. In the case of right-handed slepton mixing, we have,

$$g_{1\alpha 1}^L \simeq 0, \quad g_{1\alpha 1}^R \simeq \tan\theta_W \frac{M_{R\tau}^e M_{R\alpha}^e}{M_{R\tau}^{e\ 2} - M_{R\alpha}^{e\ 2}} (\delta_{RR}^e)_{\alpha\tau}, \quad (2)$$

while in the left-handed slepton mixing case, these couplings are given

$$g_{1\alpha 1}^L \simeq \frac{1}{2} \tan\theta_W \frac{m_\tau (A_0 - \mu \tan\beta)}{M_{R\tau}^{e\ 2} - M_{L\tau}^{e\ 2}} \frac{M_{L\alpha}^e M_{R\tau}^e}{M_{R\tau}^{e\ 2} - M_{L\alpha}^{e\ 2}} (\delta_{LL}^e)_{\alpha\tau}, \quad g_{1\alpha 1}^R \simeq 0. \quad (3)$$

To analyze the effects of the presence of a non-vanishing leptonic mass insertion on the NLSP lifetime, we choose four points with different mass differences as shown in Table 1. In Fig. 2 (a), we show the lifetime of the lightest slepton, $\tau_{\tilde{l}_1}$, as a function of $(\delta_{RR}^e)_{e\tau}$, encoding the right-handed selectron-stau mixing, that we vary from 10^{-10} to 10^{-2} . We can see that the lifetime for $\delta m > m_\tau$ (case A in Table. 1) does not change, because the decay of slepton to tau and neutralino is always the dominant decay mode and the lifetime is insensitive to δ_{RR}^e ($\leq 10^{-2}$). On the other hand, for $\delta m < m_\tau$, the lifetime grows more than 13 orders of magnitude in the limit $(\delta_{RR}^e)_{e\tau} \rightarrow 0$, where the three- or four-body decay processes are dominant. Then, the two-body decay into τ and $\tilde{\chi}_1^0$ is forbidden but those into e (or μ for $(\delta_{RR}^e)_{\mu\tau} \neq 0$) and $\tilde{\chi}_1^0$ are allowed through LFV couplings. The lifetime decreases proportionally to $|(\delta_{RR}^e)_{e\tau}|^{-2}$ when the two-body decay dominates total decay width. For values of $\delta^e > 10^{-2}$ the mass of the lightest slepton would be substantially changed by this large off-diagonal entry and this would reduce the mass difference changing the simple $|(\delta_{RR}^e)_{e\tau}|^{-2}$ proportionality. This can be seen as an increase of the lifetime in the case D at $(\delta_{RR}^e)_{\mu\tau} \simeq 10^{-2}$ in Fig. 2 (b). Although $\delta_{RR}^e > 10^{-2}$ is still allowed by experiments, we concentrate our discussion on $\delta_{RR}^e \leq 10^{-2}$ to show the sensitivity of this process to small δ_{RR}^e s. In fact, from these figures we can see that the lifetime indeed has very good sensitivity to small δ^e s in this scenario. Comparing the bounds on the mass insertions given in [27] with the figures we can see that the sensitivity obtained in the measurement of the NLSP lifetime can not be reached by indirect experiments as $\tau \rightarrow \mu \gamma$ and $\tau \rightarrow e \gamma$, etc.

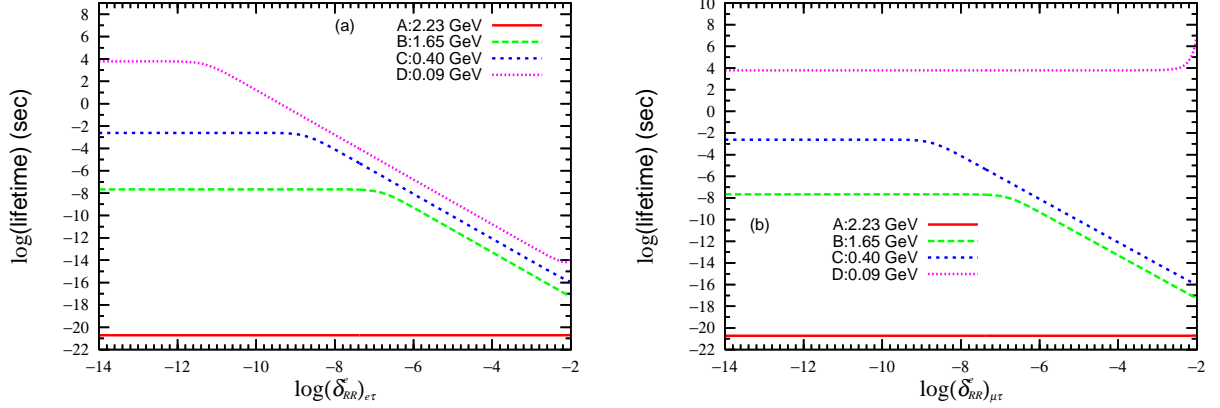


Figure 2. The lifetime of the lightest slepton as a function of δ_{RR}^e . The left panel, (a), is the lifetime of the lightest slepton with the right-handed selectron and stau mixing, and the right panel, (b), is the one with the right-handed smuon and stau mixing. In both panel, the solid (red), dashed (green), dotted (blue), dotted-dashed (pink) line correspond to the point A, B, C, D of Table. 1, respectively. $m_0 = 260$ GeV, $A_0 = 600$ GeV and $M_{1/2}$ is varied.

Plot (b) in Fig. 2 corresponds to the right-handed smuon-stau mixing, $(\delta_{RR}^e)_{\mu\tau}$. The lifetime is constant for $\delta m = 0.09$ GeV in small $(\delta_{RR}^e)_{\mu\tau}$ as the two-body decay in muon is still forbidden. For larger δm , we observe again the same dependence on $(\delta_{RR}^e)_{\mu\tau}$.

Figs. 3 (a) and (b) show the lifetime of the lightest slepton as a function of $(\delta_{LL}^e)_{e\tau}$ and $(\delta_{LL}^e)_{\mu\tau}$, respectively. The different curves correspond to the same mass differences used in Fig. 2. The dependence on these mass insertions in these figures is completely analogous to the behavior observed in Fig. 2. In fact, both figures would be identical if we replace (δ_{LL}^e) by $10 \times (\delta_{RR}^e)$. This is due to the fact that in this case, the lightest slepton decays into the electron or the muon through the left-handed stau component. The mixing of right and left-handed staus, Eq. (3), is proportional to $m_\tau(A_0 - \mu \tan \beta)/(M_{R\tau}^e - M_{L\tau}^e)$. In the region of parameter space we are considering this factor is approximately 0.1. Thus, we can see that, also in the case of (δ_{LL}^e) , the lifetime is sensitive to the presence of very small lepton flavour violating couplings and therefore to the presence of mass insertions orders of magnitude smaller than the present bounds.

4. LHC Phenomenology

In this section, we discuss the expected phenomenology at LHC experiments, focusing mainly on the ATLAS detector [29, 30], of the long-lived slepton scenario. The lightest slepton is the NLSP, and therefore a large number of sleptons is expected to be produced via cascade decays of heavier SUSY particles. When the long-lived sleptons have lifetimes between 10^{-5} and 10^{-11} sec., we will have a chance to observe decays of the slepton inside the detector. In the following, we show that, in the relevant region of SUSY parameter space, we can see decays of sleptons with the lifetime up to 10^{-5} seconds within the ATLAS detector. Although we discuss only the ATLAS detector, analysis is similar to the CMS detector [31].

First, we estimate the number of lightest sleptons produced at LHC. In our scenario, the lightest slepton is mainly a right-handed stau and the lightest neutralino is mainly bino. The

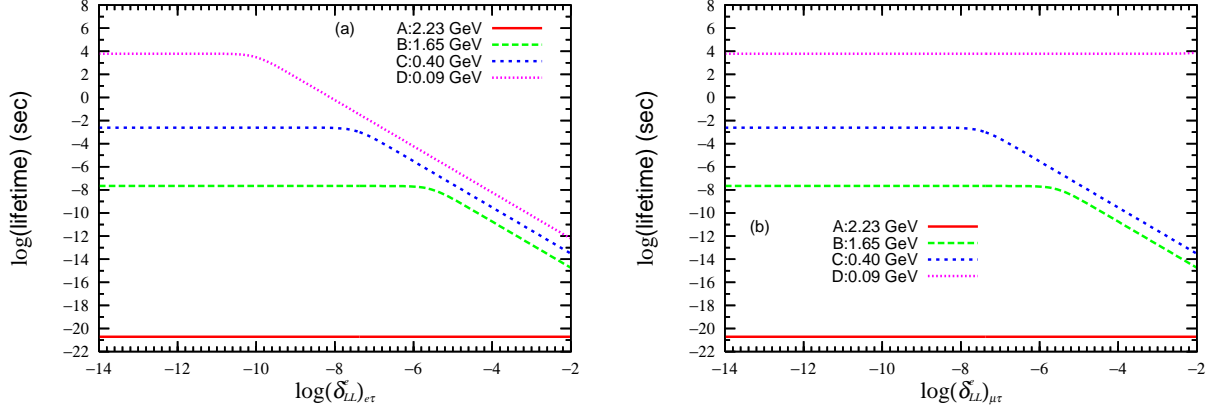


Figure 3. The lifetime of the lightest slepton as a function of δ_{LL}^e . The lines and the parameters are the same as Fig.2.

spectrum that we consider here corresponds approximately to the post-WMAP SUSY benchmark point J' proposed in [32, 33] with a slightly different $\tan \beta$ value ($\tan \beta = 35$ versus $\tan \beta = 30$ in our case). Then, the right-handed staus are mainly produced via decays of first two generation left-handed squarks. The 3rd generation squarks have many different decay chains. Total branching ratios for \tilde{l}_1 production are 0.86 in \tilde{q}_L decay, 0.72/0.90 for \tilde{t}_1/\tilde{t}_2 and 0.87/0.67 for \tilde{b}_1/\tilde{b}_2 at $\tan \beta = 35$ [32, 33, 34]. On the other hand, the right-handed squarks, couple only to bino and higgsino, having small Yukawa couplings, decay almost completely to the lightest neutralino and quarks. Therefore branching ratios of them into \tilde{l}_1 and quarks/leptons are negligible. The total cross section of SUSY pair production in our scenario is given as $\sigma_{\text{SUSY}} = 130 \text{ fb}$ in [35]¹. When we assume the integrated luminosity, $\mathcal{L}_{\text{int}} = 30 \text{ fb}^{-1}$, the total number of SUSY pairs is 3900. Then, squarks are pair-produced with equal probability for left and right-handed squarks, thus, the number of lightest sleptons produced, $N_{\tilde{l}_1}$, is estimated as $N_{\tilde{l}_1} \simeq 4290$. To obtain the expected number of decays, we need to know the distribution of $\beta\gamma$ where $\beta = v/c$ and $\gamma = 1/\sqrt{1-\beta^2}$ with c the speed of the light. This would require a full analysis with Monte-Carlo simulation and it is beyond the scope of this paper. For the spectrum we consider, the typical momentum of the lightest slepton is expected to be between 500 and 900 GeV. $\beta\gamma$ corresponding to this range of momenta is $1.53 \lesssim \beta\gamma \lesssim 2.75$, hence we can assume $\beta\gamma$ to be 2.

In Table 2, we show the expected number of slepton decays in each detector, assuming the integrated luminosity, $\mathcal{L}_{\text{int}} = 30 \text{ fb}^{-1}$ and $\beta\gamma = 2$. As can be seen, when the lifetime, $\tau_{\tilde{l}_1}$, is below 10^{-9} sec. , most of the sleptons decay inside the pixel detector. When $\tau_{\tilde{l}_1} \sim 10^{-8} \text{ sec.}$, almost half of them decay inside the inner detector and nearly all of them decay within the detector. If $\tau_{\tilde{l}_1}$ is between 10^{-8} and 10^{-6} sec. , several hundreds of slepton decays occur inside the ATLAS detector. Almost all of them escape from the detector when $\tau_{\tilde{l}_1} > 10^{-5} \text{ sec.}$, although we expect of the order of 10 decays inside the detector for $\tau_{\tilde{l}_1} \simeq 10^{-5} \text{ sec.}$

Sleptons with different lifetimes would give different signatures in the ATLAS detector. Depending on the lifetimes, sleptons would decay inside the detector or escape the detector as a stable heavy charged-particle. For $\tau_{\tilde{l}_1} < 10^{-11} \text{ sec.}$, since almost all of the sleptons would

¹ Taking into account that the production cross section is almost identical for different values of $\tan \beta$, we use the cross section for point $P_2 \simeq J'$ in [35]

Table 2. The expected number of slepton decay in the ATLAS detector. The length is the minimum (5 cm) and medium (50 cm) distance to the pixel detector and the maximum distance to the outer boundary of the detectors from the interaction point and corresponds to pixel detector (3.1 m), calorimeter (5.8 m) and muon spectrometer (25.0 m). The lifetime is varied from 10^{-11} to 10^{-5} seconds. $\beta\gamma$ is fixed to 2.

	5 cm	50 cm	3.1 m	5.8 m	25.0 m
10^{-5} sec.	0.04	0.36	2.2	4.1	17.8
10^{-6} sec.	0.36	3.6	22.1	41.3	175.1
10^{-7} sec.	3.6	35.6	216.0	395.3	1461.9
10^{-8} sec.	35.6	343.0	1731.0	2658.3	4223.5
10^{-9} sec.	343.0	2425.6	4265.5	4289.7	4290.0
10^{-10} sec.	2425.6	4289.0	4290.0	4290.0	4290.0
10^{-11} sec.	4289.0	4290.0	4290.0	4290.0	4290.0

decay before they reach the first layer of the pixel detector, we would not observe any heavy charged-particle track in the detector. In this case, it would be more difficult to identify the presence of long-lived sleptons at the ATLAS detector. This problem will be addressed in a future work [36]. For $\tau_{\tilde{l}_1} \sim 10^{-10}$ to 10^{-9} sec, almost all the sleptons would decay inside the pixel detector and leave a charged track with a kink. Then, a different charged-particle would cross the outer detectors and a corresponding track and/or hit would be seen in each detector. Thus, by combining with signals in the outer detectors, we could identify whether the outgoing charged-particle is an electron or muon. Then, if we can fix the mass difference between the lightest slepton and neutralino, we can determine the value of the mass insertion parameters from Figs. 2 and 3. In the case of right-handed slepton mixing case, lifetimes between 10^{-10} and 10^{-8} sec. would correspond to $(\delta_{RR}^e)_{e\tau}$ between 10^{-7} and 10^{-4} with the mass difference, $m_e < \delta m < m_\tau$, and $(\delta_{RR}^e)_{\mu\tau}$ between 10^{-7} and 10^{-5} with $m_\mu < \delta m < m_\tau$. Similarly, in the case of left-handed slepton mixing, the same lifetimes would correspond to $(\delta_{LL}^e)_{e\tau}$ between 4×10^{-6} and 10^{-3} with $m_e < \delta m < m_\tau$, and $(\delta_{LL}^e)_{\mu\tau}$ between 4×10^{-6} and 10^{-4} with $m_\mu < \delta m < m_\tau$. For $\tau_{\tilde{l}_1} \sim 10^{-8}$ sec., about half of sleptons would decay inside the inner detector and the rest would decay inside the calorimeters and/or muon spectrometer. In this case, it would be important to determine whether the decay is LFV two-body decay or lepton flavour conserving three-body decay [36]. For lifetimes between 10^{-7} and 10^{-5} sec., very few sleptons would decay inside the pixel detector and most of them would escape the detector leaving a charged track with a corresponding hit in muon spectrometer. Even for particles escaping the detector, we could use muon spectrometer to determine slepton mass and momentum as studied in [19, 20]. For $\tau_{\tilde{l}_1} \gtrsim 10^{-5}$ sec., very few sleptons would decay inside the ATLAS detector. In this case, we can put lower bound on the lifetime. Then, in a gravity-mediated scenario, this would correspond to a stringent upper bound on δ^e s.

This scenario of long-lived slepton is in principle similar to the situation in gauge-mediated SUSY breaking scenario [21]. For similar lifetimes, more detailed analysis is needed to distinguish scenarios. However most of sleptons in gauge-mediated SUSY breaking scenario would escape from the detector and we could see only a few events.

5. Summary

In this work, we have studied lepton flavour violation in a long-lived slepton scenario where the mass difference between the NLSP, the lightest slepton, and the LSP, the lightest neutralino, is smaller than the tau mass. With this small mass difference, the lifetime of the lightest slepton has a very good sensitivity to small lepton flavour violation parameters due to the more than 13 orders of magnitude suppression of the three-body decay rate with respect to the two-body decay rate.

We have shown that this small δm is possible even in the framework of the CMSSM. We selected the region in the CMSSM parameter space with $\delta m < m_\tau$, taking into account correct dark matter abundance and direct bounds on SUSY and Higgs masses and $b \rightarrow s \gamma$ constraint. We have used the experimental results of the anomalous magnetic moment of the muon to indicate the favored regions at given confidence level. We have found that a small δm region consistent with all experimental constraints lies on sizable part of the parameter space at $M_{1/2} \gtrsim 700$ GeV, $m_0 = 100$ to 600 GeV for different values of $\tan \beta$. We have also shown that the most favored region, which is consistent with a_μ at 2σ , corresponds to $240 \lesssim m_0 \lesssim 260$ GeV and $700 \lesssim M_{1/2} \lesssim 800$ GeV at $\tan \beta = 35$.

Then, we have analyzed the dependence of the lightest slepton lifetimes on different mass insertions, $(\delta_{RR/LL}^e)_{e\tau, \mu\tau}$ for values of δm from 2.23 to 0.09 GeV. We found that the lifetimes are proportional to $|\delta^e|^{-2}$ until three- or four-body decays become comparable. There is a difference of approximately a factor of 10 in the sensitivity of the lifetime on δ_{RR}^e and δ_{LL}^e . This is due to the different proportion of left-handed and right-handed staus in the lightest slepton. By comparing the values of the bounds on δ^e s shown in [27], we can see that, in this scenario, the lifetimes are sensitive to much smaller values of these δ^e s, even to future sensitivities of proposed experiments.

Finally, we have discussed the expected phenomenology at LHC experiments, mainly concentrating on the ATLAS detector. We have estimated the number of slepton decays in the different detectors, assuming an integrated luminosity $\mathcal{L}_{\text{int}} = 30 \text{ fb}^{-1}$ and $\beta\gamma = 2$ (Table. 2). We have seen that the ATLAS detector can observe lifetimes in the range of 10^{-11} to 10^{-6} sec., and these lifetime would correspond to $(\delta_{RR}^e)_{e\tau, \mu\tau}$ between 10^{-7} and 10^{-3} and $(\delta_{LL}^e)_{e\tau, \mu\tau}$ between 4×10^{-6} and 10^{-3} . Therefore we have shown that in the long-lived slepton scenario, the LHC offers a very good opportunity to study lepton flavour violation.

Acknowledgments

The authors, O. V. and T. S., would like to thank V. Mitsou for fruitful discussion on detection possibilities of the long-lived slepton at the ATLAS detector, and J. Jones-Perez for numerical checks of bounds on mass insertions. S.K. was supported by European Commission Contracts MRTN-CT-2004-503369 and ILIAS/N6 WP1 RI I3-CT-2004-506222, and also Fundação para a Ciência e a Tecnologia (FCT, Portugal) through CFTP-FCT UNIT 777 which is partially funded through POCTI (FEDER). S.K. is an ER supported by the Marie Curie Research Training Network MRTN-CT-2006-035505. The work of J. S. was supported in part by the Grant-in-Aid for the Ministry of Education, Culture, Sports, Science, and Technology, Government of Japan Contact Nos. 20025001, 20039001, and 20540251. The work of T. S. and O. V. was supported in part by MEC and FEDER (EC), Grants No. FPA2005-01678 and the Generalitat Valenciana for support under the grants PROMETEO/2008/004, GV05/267 and GVPRE/2008/003. The work of O. V. was also supported in part by European program MRTN-CT-2006-035482 “Flavianet”.

The work of M. Y. was supported in part by the Grant-in-Aid for the Ministry of Education, Culture, Sports, Science, and Technology, Government of Japan (No. 20007555).

References

- [1] Griest K and Seckel D, *Phys. Rev. D* **43** (1991) 3191.
- [2] Jittoh T, Sato J, Shimomura T and Yamanaka M, *Phys. Rev. D* **73**, 055009 (2006) [arXiv:hep-ph/0512197].
- [3] Jittoh J, Kohri K, Koike M, Sato J, Shimomura T and Yamanaka M, *Phys. Rev. D* **76**, 125023 (2007) [arXiv:0704.2914 [hep-ph]].
- [4] Jittoh T, Kohri K, Koike M, Sato J, Shimomura T and Yamanaka M, *Phys. Rev. D* **78**, 055007 (2008) [arXiv:0805.3389 [hep-ph]].
- [5] Ryan S G, Beers T C, Olive K A, Fields B D and Norris J E, *Astrophys. J.* **530** (2000) L57.
- [6] Cyburt R H, Fields B D and Olive K A, *Phys. Lett. B* **567**, 227 (2003) [arXiv:astro-ph/0302431].
- [7] Coc A, Vangioni-Flam E, Descouvemont P, Adahchour A and Angulo C, *Astrophys. J.* **600**, 544 (2004) [arXiv:astro-ph/0309480].
- [8] Jarosik N *et al.* [WMAP Collaboration], *Astrophys. J. Suppl.* **170**, 263 (2007) [arXiv:astro-ph/0603452].
- [9] Dunkley J *et al.* [WMAP Collaboration], arXiv:0803.0586 [astro-ph].
- [10] Agashe K and Graesser M, *Phys. Rev. D* **61** (2000) 075008 [arXiv:hep-ph/9904422].
- [11] Deppisch F, Pas H, Redelbach A, Ruckl R and Shimizu Y, *Phys. Rev. D* **69** (2004) 054014 [arXiv:hep-ph/0310053].
- [12] Deppisch F, Kalinowski F, Pas H, Redelbach A and Ruckl R, arXiv:hep-ph/0401243.
- [13] Bartl A, Hidaka K, Hohenwarter-Sodek K, Kernreiter T, Majerotto W and Porod W, *Eur. Phys. J. C* **46** (2006) 783 [arXiv:hep-ph/0510074].
- [14] Ibarra A and Roy S, *JHEP* **0705** (2007) 059 [arXiv:hep-ph/0606116].
- [15] Hohenwarter-Sodek K and Kernreiter T, *JHEP* **0706** (2007) 071 [arXiv:0704.2684 [hep-ph]].
- [16] Hirsch M, Valle J W F, Porod W, Romao J C and Villanova del Moral A, arXiv:0804.4072 [hep-ph].
- [17] Hirsch M, Kaneko S and Porod W, arXiv:0806.3361 [hep-ph].
- [18] Hamaguchi K, Nojiri M M and de Roeck A, *JHEP* **0703**, 046 (2007) [arXiv:hep-ph/0612060].
- [19] Tarem S *et al.* [ATLAS Collaboration] ATL-SN-ATLAS-2008-071
- [20] Tarem S *et al.* ATL-PHYS-PUB-2005-02
- [21] Ishiwata K, Ito T and Moroi T, arXiv:0807.0975 [hep-ph].
- [22] Porod W, *Comput. Phys. Commun.* **153**, 275 (2003) [arXiv:hep-ph/0301101].
- [23] Belanger G, Boudjema F, Pukhov A and Semenov A, arXiv:0803.2360 [hep-ph].
- [24] Bennett G W *et al.* [Muon G-2 Collaboration], *Phys. Rev. D* **73**, 072003 (2006) [arXiv:hep-ex/0602035].
- [25] Davier M, *Nucl. Phys. Proc. Suppl.* **169**, 288 (2007) [arXiv:hep-ph/0701163].
- [26] Ellis J R, Falk T, Olive K A and Srednicki M, *Astropart. Phys.* **13** (2000) 181 [Erratum-ibid. **15** (2001) 413] [arXiv:hep-ph/9905481].
- [27] Kaneko S, Sato J, Shimomura T, Vives O and Yamanaka M, *Phys. Rev. D* **78**, 116013 (2008) [arXiv:0811.0703 [hep-ph]].
- [28] Masina I and Savoy C A, *Nucl. Phys. B* **661**, 365 (2003) [arXiv:hep-ph/0211283].
- [29] Bentvelsen S *et al.* [ATLAS Collaboration], *JINST* **3** (2008) S08003
- [30] For more information on the ATLAS Experiment, visit website <http://atlas.ch/>
- [31] Adolphi A *et al.* [CMS Collaboration], *JINST* **3** (2008) S08004
- [32] Battaglia M *et al.*, *Eur. Phys. J. C* **22**, 535 (2001) [arXiv:hep-ph/0106204].
- [33] Battaglia M, De Roeck A, Ellis J R, Gianotti F, Olive K A and Pape L, *Eur. Phys. J. C* **33**, 273 (2004) [arXiv:hep-ph/0306219].
- [34] For different values of $\tan\beta$, branching ratios for each decay are different but total branching ratio will be the same.
- [35] Skands P Z, *Eur. Phys. J. C* **23**, 173 (2002) [arXiv:hep-ph/0110137].
- [36] Kaneko S, Sato J, Shimomura T, Vives O and Yamanaka M, work in progress.